Master Equation, Design Equations and Runaway Speed of the Kaplan Turbine

Zh. Zhang
ZHAW, Zurch University of Applied Science, Zurich, Switzerland
E-mail: zhengji.zhang@hotmail.com

Abstract

To make the Kaplan turbine technology comparable to both the Pelton and the Francis turbine, the master equation for the Kaplan turbine has been established by following similar analyses as for the Francis turbine. The analysis begins with the descriptions of free vortex flows at the runner inlet and the swirl flow at the impeller exit. By considering the Euler equation for specific work and by further evaluating the most significant shock and swirling losses, the *first* and the *second energy equations* in the form of hydraulic efficiency were formulated. The master equation is then established by combining both energy equations. In addition, three design equations and a new design parameter are presented.

The master equation relates the turbine hydromechanics to the geometrical design of both the runner and the guide-vane parameters. It enables the complete hydraulic characteristics of a given Kaplan turbine to analytically and simply be computed. A computation example demonstrates the functionality and applicability of the method. With the reconstructed master equation, the runaway speed of the Kaplan turbine and its dependence on the guide-vane setting can be easily and precisely computed.

For bulb turbines with guide vanes directly ahead of the turbine runner in the same tube, all computations are also applicable using another equivalent control parameter.

Keywords: Kaplan turbine, master equation, design equations, design parameter, runaway speed, hydraulic efficiency, shock loss, swirling loss, bulb turbines

Introduction

The Kaplan turbine is an important type of water turbines in hydroelectric power plants. It ranks third behind the Pelton and Francis turbines. The three turbines share the properties that they all can be well designed, manufactured and operated for high hydraulic performances, based on developments and experiences over the past 100 years. In view of hydromechanical fundamentals, both the Pelton and the Francis turbines have been greatly developed in recent years [1, 2]. The respective main and master equations enable the hydraulic characteristics to be accurately computed up to the runaway speed. In comparison, the Kaplan turbine is clearly underdeveloped, so that comparable hydraulic characteristics are still not obtainable by computations. All data and diagrams currently used in design and operations are mainly based on measurements and empirical relations.

One finds the design rules for Kaplan turbines, for instance, in [3-6]. All these rules are clearly referred to the nominal operation, i.e., the best efficiency point (BEP). One also likely confirms that such design rules have hardly progressed in the past more than half century. Almost all investigations found in the past thirty years are case studies that are restricted to either model tests or numerical simulations by CFD. Some of them are mainly focused on special issues like cavitation, hydraulic vibration, rotor-stator interactions, and abrasive erosion [7]. As consequence, no noticeable hydromechanical relations in the Kaplan turbine could be found. In addition, the study of hydrodynamics of the Kaplan turbine also seems to be lagging, if compared to the Francis turbine [8, 9].

In some other investigations [10-12], flow distributions both upstream (as in a spiral case and distributer) and downstream (as in a draft tube) of the Kaplan turbine have been characterised. The knowledge about such flow distributions helps to make hypotheses for further analyses, like the potential flow models.

The Kaplan turbine is a reaction turbine, comparable to the Francis turbine. In view of the creation of the master equation of the Francis turbine [2], it should be possible to create a similar equation for the Kaplan turbine by following similar computations. As required, this again relies on the application of laws of energy and angular momentum (Euler) which governs the flows in the Kaplan turbine. When applying the energy law, one obviously needs to quantify all existing losses in the turbine system. These mainly include the viscous friction loss, the shock loss at the runner inlet, and the swirling loss at the runner exit; the last two occur in off-design operations.

The attempt to make flow analyses and to create the master equation of the Kaplan turbine is of great significance that many accurate statements about the hydraulic performances of the

Kaplan turbine can be made. As for the Francis turbine [2], the master equation, for instance, provides a very reliable method for computations of the runaway speed, for which laboratory tests are too expensive and CFD simulations are too inaccurate and unreliable.

For convenience of the reader, similar approaches as in [2] for the Francis turbine will be applied. They basically focus on two energy equations: Euler's equation for the specific work and the energy balance accounting for all significant losses. Based on accurate formulations of these two equations and by combining them, the master equation will be obtained, from which the entire hydraulic characteristics including the runaway speed of the Kaplan turbine can be further computed. The computational scheme is illustrated in Fig. 1.

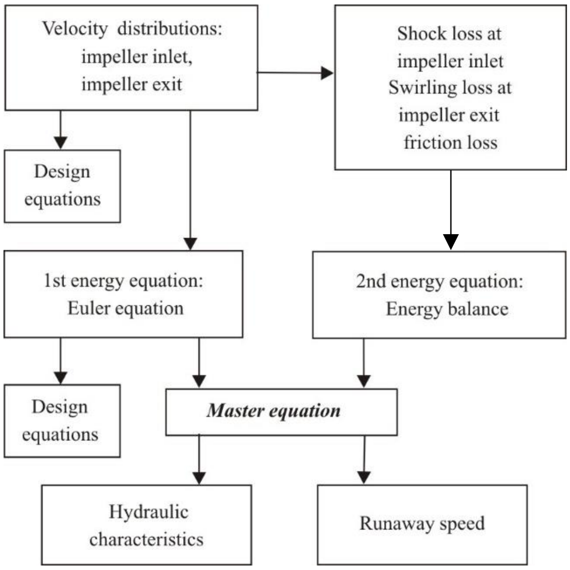

Fig. 1 Computational scheme for creation of the master equation and design equations of the Kaplan turbine

Because the complete characteristics of a Kaplan turbine also include the variation of the rotational speed, the definition of the nominal operation point of the Kaplan turbine needs to be extended, as described in the next section.

To limit the length of this manuscript, we only discuss Kaplan turbines with fixed runner blades, as shown in Fig. 2. The wicked gate (guide vanes) in its position causes radial and circumferential velocity components. The discharge, i.e., the turbine load is commonly governed by the guide-vane setting. For Kaplan turbines with guide vanes close to the runner, i.e., in the same tube (bulb turbine for instance), all analyses are still applicable; only one needs to use an equivalent control parameter for load regulation. This will be presented in Sect. 4.

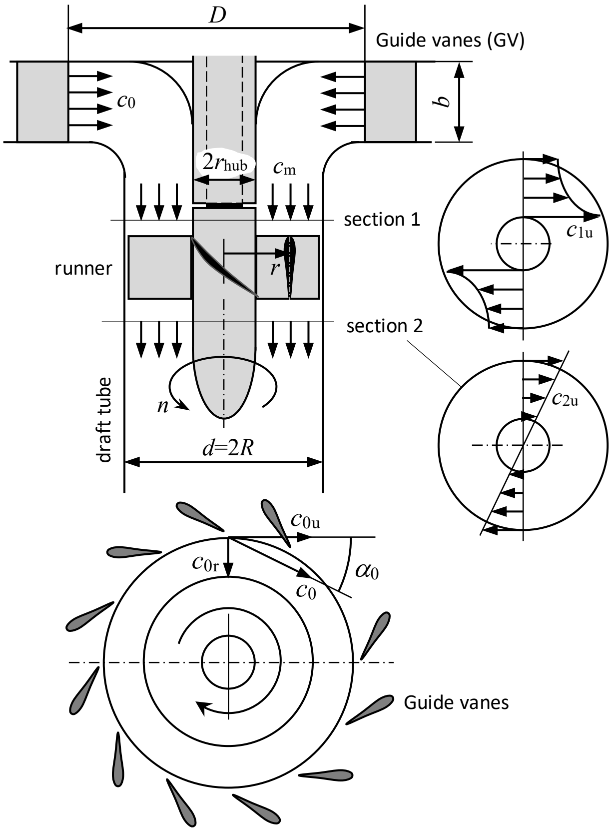

Fig. 2 Kaplan turbine and velocity distributions

1 Flow Mechanical Analysis

1.1 Extension of the Nominal Operation Condition

Each Kaplan turbine is designed for a given nominal, i.e., rated operating point which is specified by the nominal head, the nominal discharge and the nominal rotational speed. The last is usually fixed to the synchronous speed of the generator and, thus, determined by the line frequency and the pole pair number of the generator. The designed operation condition ensures the maximum hydraulic efficiency and is realised by the shockless flow at the runner inlet ($\beta_{1,\mathrm{N}}=\beta_{1\mathrm{b}}$ in Fig. 3 with $\beta_{1\mathrm{b}}$ as the design angle of the runner blade at the runner inlet) and the non-swirling flow at the runner exit ($\alpha_{2,\mathrm{N}}=\pi/2$). Deviations from the designed operating point are encountered, for instance, by the season-dependent height of water in the lake or by changing the guide-vane angle to regulate the discharge (turbine load).

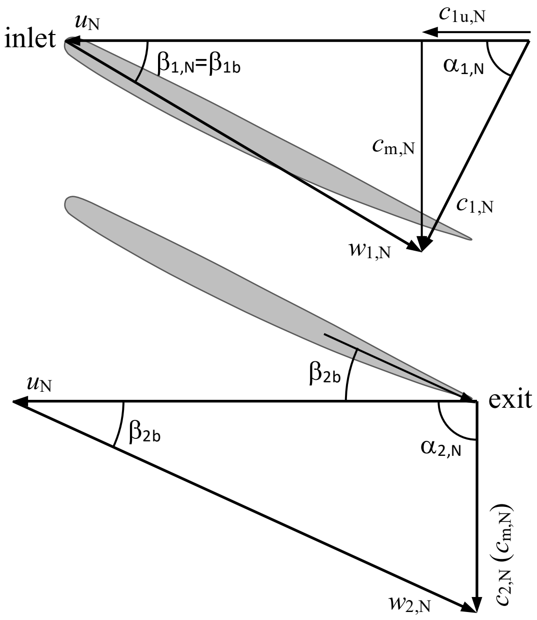

Fig. 3 Velocity triangles at the runner inlet and exit under the nominal operating condition

The complete hydraulic performance of a Kaplan turbine also accounts for the case of changeable rotational speed. This is not only to respond to the change in water level in the lake (for optimum hydraulic efficiency), it is also related to the hydraulic transients, which occur either during the start-up of the turbine or in the case of load rejection leading to a speed-up of the turbine towards the runaway speed. Because of its significance, the definition of the nominal operation condition of the Kaplan turbine must be extended to include both the changeable head and the varying rotational speed. This simply means that for each given head there exists a new fictitious nominal operating point that is specified by the speed and the discharge. On the other hand, turbine operations with varying speed have also been well established in practical applications. For this reason and to extend the nominal operation conditions, the following dimensionless *unit parameters* for rotational speed, discharge, and hydraulic torque, respectively, have been commonly defined:

$$n_{11}=\frac{\pi dn}{\sqrt{2gH}}, \quad \dot{Q}_{11}=\frac{\dot{Q}}{d^2\sqrt{2gH}}, \quad M_{11}=\frac{M_{\text{hyd}}}{\rho d^3\left(gH\right)} \tag{1}$$

Here H and d state for the total pressure head and runner diameter, respectively.

For the purpose of graphical presentation of the shaft power, the unit power or the power coefficient is defined, with respect to $P_{\text{hyd}}=2\pi nM_{\text{hyd}}$, as follows:

$$\lambda_{11}=\frac{P_{\text{hyd}}}{\rho d^2\left(2gH\right)^{3/2}}=n_{11}M_{11} \tag{2}$$

It is a derived variable (non-independent).

In above definitions, n is in 1/s and $\dot{Q}$ in m^3/s. ρ is the density of water. The runner diameter d is used for the characteristic length. It is supposed to be equal to the tube diameter (Fig. 2).

Furthermore, with u_{d} as the peripheral speed of the runner, both the discharge and the head coefficients are defined as

$$\varphi = \frac{\dot{Q}}{u_{\mathrm{d}}\, \pi d^2/4} = \frac{4\dot{Q}}{\pi^2 d^3 n} \tag{3}$$

$$\psi = \frac{2gH}{u_{\mathrm{d}}^2} = \frac{2gH}{(\pi d n)^2} \tag{4}$$

The definition of the head coefficient is equivalent to the unit speed because of $\psi = 1/n_{11}^2$. The use of n_{11} against ψ in Kaplan turbines, however, is favourable because the case of n=0 can be well interpreted by $n_{11} = 0$.

According to the definitions in Eq. (1), corresponding values under nominal operation conditions are denoted as $n_{11,\mathrm{N}}$, $\dot{Q}_{11,\mathrm{N}}$, and $M_{11,\mathrm{N}}$. Keeping these unit parameters constant simply means that to each given hydraulic head (H) there exists a new nominal operating point ($\dot{Q}_{\mathrm{N}}$, n_{N}) that is completely analogous to the design point for the designed head. The extended nominal operation condition of a Kaplan turbine is thus implemented by additionally accounting for the variable head. The term "nominal", instead of "rated" or "designed", is used to generally represent the best efficiency point (BEP) of the Kaplan turbine, which operates with variable head and speed.

Correspondingly, the *nominal discharge coefficient* is given as

$$\varphi_{\mathrm{N}} = \frac{4\dot{Q}_{\mathrm{N}}}{\pi^2 d^3 n_{\mathrm{N}}} \tag{5}$$

From Eqs. (1) and (5), one obtains

$$\varphi_{\mathrm{N}} = \frac{4}{\pi} \frac{\dot{Q}_{11,\mathrm{N}}}{n_{11,\mathrm{N}}} \tag{6}$$

The nominal discharge coefficient φ_{N} is a specification parameter of a Kaplan turbine. Its application in the current paper contributes to the simplification of some computational results.

1.2 Runner Design and Flow Distributions

Based on given nominal values of head, discharge and rotational speed, the specific speed of the Kaplan turbine is defined as

$$n_{\mathrm{q}} = n_{\mathrm{N}} \frac{\sqrt{\dot{Q}_{\mathrm{N}}}}{H_{\mathrm{N}}^{3/4}} \tag{7}$$

It is a design parameter which basically determines the geometrical form of the turbine runner.

In the practical design of the Kaplan turbine up to now, the head coefficient ψ_{N} has been arranged as a function of the specific speed n_{q}. With respect to $\psi_{\mathrm{N}} = 1/n_{11,\mathrm{N}}^2$ and n_{11} definition according to Eq. (1), the diameter of the runner d can be determined (in [3], for instance, notation k_{u} is used in place of n_{11}). For other parameters, empirical equations and diagrams as a function of n_{q} can be found in the literature.

A brief review of the specific speed defined in Eq. (7) should be given. As a design parameter, the specific speed exactly determines all relevant geometrical design and operational parameters of the Pelton turbine [1]. It is, however, not accurate for the Kaplan turbine in geometrical configurations. As will be shown below in Sect. 1.5, a new parameter seems to be much applicable than the specific speed.

1.2.1 Flow Distribution at the Runner Inlet

The flow from the upper reservoir, through the wicket gate, to the inlet of the turbine runner is only subject to the viscous friction effect. It can thus be assumed to be a type of the potential flow with free vortex distributions. According to Fig. 2, the volume flow rate $\dot{Q}$ is regulated by guide vanes (the wicket-gate height is b). If the flow angle is set to be α_0, the rate of angular momentum of the flow is computed as (with the flow area $A_0 = \pi D b$ and the volume flow rate $\dot{Q} = c_{0\mathrm{r}} A_0$)

$$\dot{L}_0 = c_{0\mathrm{u}} \frac{D}{2} \rho \dot{Q} = \frac{c_{0\mathrm{r}}}{\tan \alpha_0} \frac{D}{2} \rho \dot{Q} = \frac{1}{\tan \alpha_0} \frac{1}{2\pi b} \rho \dot{Q}^2 \tag{8}$$

This value remains in the approaching flow at the runner inlet (cross-section 1) with uniform distribution of the meridian (axial) velocity component (c_{m}). It is also independent of the wicket-gate diameter D. Because the flow can be assumed to be free of any energy loss, its distribution in the cross-section at the runner inlet must satisfy the condition of free vortex flows (potential flows), so that for the circumferential velocity component in function of radial coordinate r

$$c_{1u} = c_{1u,hub} \frac{r_{hub}}{r} \tag{9}$$

The velocity component $c_{1u,hub}$ on the hub surface is yet unknown. The associated angular momentum is then computed with $d\dot{Q} = 2\pi r c_m dr$ and $\dot{Q} = \pi\left(R^2 - r_{hub}^2\right)c_m$ as

$$\dot{L}_1 = \rho \int_0^{\dot{Q}} c_{1u} r d\dot{Q} = 2\pi\rho c_m c_{1u,hub} r_{hub} \int_{r_{hub}}^{R} r dr = \rho \dot{Q} c_{1u,hub} r_{hub} \tag{10}$$

By equalizing Eqs. (8) and (10), the term $c_{1u,hub} r_{hub}$ can be obtained which is then inserted into Eq. (9), leading to the flow distribution at the runner inlet

$$c_{1u} = \frac{R}{r} \frac{c_m}{\tan\alpha_0} \frac{R}{2b}\left(1 - \frac{r_{hub}^2}{R^2}\right) \tag{11}$$

When considering the velocity triangle at the runner inlet according to Fig. 4 (for partial load for instance), the relative velocity is given by

$$w_1^2 = c_m^2 + \left(u - c_{1u}\right)^2 \tag{12}$$

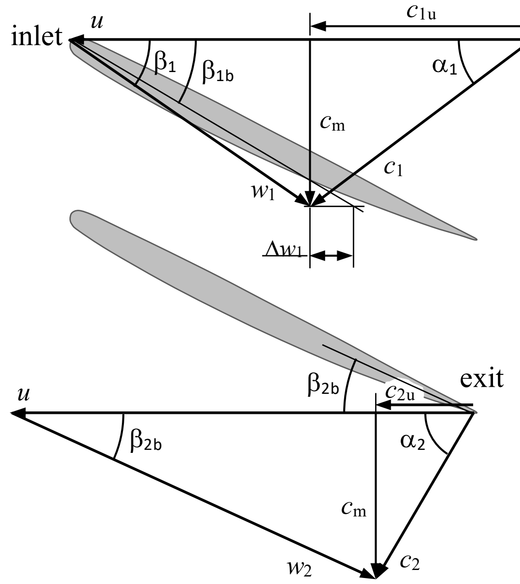

Fig. 4 Velocity triangles at the runner inlet and exit under the partial load

The relative flow angle β_1 is obtainable from

$$\frac{1}{\tan\beta_1} = \frac{u - c_{1u}}{c_m} = \frac{2\pi r n}{\dot{Q}/A} - \frac{1}{r} \frac{1}{\tan\alpha_0} \frac{R^2}{2b}\left(1 - \frac{r_{hub}^2}{R^2}\right) \tag{13}$$

With respect to Eq. (1) and the flow area $A = \pi\left(R^2 - r_{hub}^2\right)$, it is further written as

$$\frac{1}{\tan\beta_1} = R^2\left(\frac{2\pi r}{d^3}\frac{n_{11}}{\dot{Q}_{11}} - \frac{1}{2br}\frac{1}{\tan\alpha_0}\right)\left(1-\frac{r_{\mathrm{hub}}^2}{R^2}\right) \tag{14}$$

The relative flow angle has thus been shown as a function of radial coordinate *r*.

Under the nominal operating condition, this flow angle must agree with the blade angle of the turbine runner on the leading edge $\beta_{1,\mathrm{N}} = \beta_{1\mathrm{b}}$ (Fig. 3). With respect to Eq. (6) and with d=2R, one further obtains from Eq. (14) for the nominal operation

$$\frac{1}{\tan\beta_{1\mathrm{b}}} = \left(\frac{1}{\varphi_{\mathrm{N}}}\frac{r}{R} - \frac{R^2}{2br}\frac{1}{\tan\alpha_{0,\mathrm{N}}}\right)\left(1-\frac{r_{\mathrm{hub}}^2}{R^2}\right) \tag{15}$$

This equation can be used as a *design equation* for configuring the blade profile along the blade leading edge. The blade angle on the hub surface ($r = r_{\mathrm{hub}}$) reaches its maximum, and the corresponding blade angle must fulfill $\beta_{1\mathrm{b,hub}} < 90°$. Because this implies that the r.h.s of Eq. (15) is positive, the following condition must be fulfilled, when substituting φ_{N} by Eq. (5)

$$br_{\mathrm{hub}}^2 \tan\alpha_{0,\mathrm{N}} > \frac{1}{4\pi^2}\frac{\dot{Q}_{\mathrm{N}}}{n_{\mathrm{N}}} \tag{16}$$

By knowing two nominal operation parameters $\dot{Q}_{\mathrm{N}}$ and n_{N}, specifying the geometrical design of a Kaplan turbine is now possible. The above equation, thus, represents a design rule. Its equivalence, for pre-information, is given as

$$u_{\mathrm{hub,N}}^2 > gH\,, \tag{17}$$

with $u_{\mathrm{hub,N}}$ as the peripheral speed of the hub under the nominal rotational speed.

The relation which has been applied for obtaining this condition is found below in Sect. 1.5 in connection with the *first design equation* of the Kaplan turbine.

In view of Eq. (15), the nominal operation point of a Kaplan turbine is obviously uniquely determined by the guide-vane angle $\alpha_{0,\mathrm{N}}$. Any deviation of the guide-vane angle from the nominal setting $\alpha_{0,\mathrm{N}}$ will lead to a deviation of the relative flow angle β_1 from the blade angle $\beta_{1\mathrm{b}}$. This, in turn, leads to the occurrence of the shock loss (see below Sect. 1.7.2). This circumstance is the same as that with guide-vane settings in the Francis turbine [2].

The pressure distribution in cross-section 1 (Fig. 2), with assumptions of constant total pressure and uniform meridian velocity, is determined by Bernoulli equation

$$p_1 - p_{1,\mathrm{hub}} = \frac{1}{2}\rho\left(c_{1\mathrm{u,hub}}^2 - c_{1\mathrm{u}}^2\right) \tag{18}$$

Here, c_{1u}, in relation with Eq. (11), is a function of the radial coordinate r.

One confirms that the flow distribution in the cross-section at the runner inlet is completely determined by the guide-vane opening. The guide-vane angle α_0, therefore, behaves as a control parameter for load regulation in each considered Kaplan turbine.

1.2.2 Flow Distribution at the Runner Exit

The flow out of the runner and before entering the draft tube (Fig. 2) is determined by the trailing-edge profile of the runner blades. Under the nominal operating condition (Fig. 3), the exit flow is specified by vanishing circumferential velocity component, i.e., $c_{2u,N} = 0$. This is satisfied by setting the trailing edge angle β_{2b} of the runner blades as follows

$$\tan\beta_{2b} = \frac{c_{m,N}}{u_N} = \frac{c_{m,N}}{2\pi n_N}\frac{1}{r} \tag{19}$$

In this equation, the same meridian velocity component as at the runner inlet has been applied.

With respect to Eq. (5) and because of $\dot{Q}_N = c_{m,N} A$, the above equation is further written as

$$\tan\beta_{2b} = \frac{\varphi_N}{1 - r_{hub}^2/R^2}\frac{R}{r} \tag{20}$$

Obviously, it is a function of the radial coordinate r. This equation serves to configure the trailing edge profile of runner blades for a given nominal discharge. It can thus be considered as a *design equation*.

At other operation points deviating from the nominal operating condition, the exit flow out of the runner possesses a circumferential velocity component, although it is still congruent with the blade profile ($\beta_2 = \beta_{2b}$). According to Fig. 4, one obtains

$$c_{2u} = u - \frac{c_m}{\tan\beta_{2b}} = u - \frac{c_m}{c_{m,N}} u_N = 2\pi n\left(1 - \frac{n_N}{n}\frac{\dot{Q}}{\dot{Q}_N}\right) r \tag{21}$$

It is linearly proportional to the radial coordinate r and represents a flow rotation like a solid disc, as illustrated in Fig. 2.

The relative velocity w_2 can be determined using

$$w_2^2 = c_m^2 + \left(u - c_{2u}\right)^2 \tag{22}$$

On the other hand, the pressure distribution at the runner exit is non-uniform. It can be determined from the Bernoulli equation by using the relative velocity (w) and the peripheral speed (u) as

$$p_2 + \frac{1}{2}\rho\left(w_2^2 - u^2\right) = p_1 + \frac{1}{2}\rho\left(w_1^2 - u^2\right) \tag{23}$$

In this equation, the same peripheral speed u has been used, based on the assumption of quasi-axial flow through the runner.

For $r=r_{\text{hub}}$ on the hub-surface of the runner, it follows

$$p_{2,\text{hub}} + \frac{1}{2}\rho w_{2,\text{hub}}^2 = p_{1,\text{hub}} + \frac{1}{2}\rho w_{1,\text{hub}}^2 \tag{24}$$

Combining the two equations yields

$$p_2 - p_{2,\text{hub}} = p_1 - p_{1,\text{hub}} + \frac{1}{2}\rho\left(w_1^2 - w_{1,\text{hub}}^2\right) - \frac{1}{2}\rho\left(w_2^2 - w_{2,\text{hub}}^2\right) \tag{25}$$

The pressure distribution $p_1 - p_{1,\text{hub}}$ will be replaced by Eq. (18). One then obtains

$$\frac{p_2 - p_{2,\text{hub}}}{\rho/2} = \left(c_{1\text{u,hub}}^2 - c_{1\text{u}}^2\right) + \left(w_1^2 - w_{1,\text{hub}}^2\right) - \left(w_2^2 - w_{2,\text{hub}}^2\right) \tag{26}$$

From Eqs. (12) and (22), corresponding expressions $w_1^2 - w_{1,\text{hub}}^2$ and $w_2^2 - w_{2,\text{hub}}^2$ can be determined. They are then inserted into Eq. (26), yielding

$$\frac{p_2 - p_{2,\text{hub}}}{\rho/2} = c_{2\text{u,hub}}^2 - c_{2\text{u}}^2 - 2\left(u_{\text{hub}}c_{2\text{u,hub}} - uc_{2\text{u}}\right) + 2\left(u_{\text{hub}}c_{1\text{u,hub}} - uc_{1\text{u}}\right) \tag{27}$$

The last term in this equation disappears due to free vortex flow, see Eq. (9). Further, applying Eq. (21) to above equation leads to

$$\frac{p_2 - p_{2,\text{hub}}}{\rho/2} = c_{2\text{u,hub}}^2\left(1 - 2\frac{u_{\text{hub}}}{c_{2\text{u,hub}}}\right) + 4\pi^2 n^2\left(1 - \frac{n_{\text{N}}^2}{n^2}\frac{\dot{Q}^2}{\dot{Q}_{\text{N}}^2}\right)r^2 \tag{28}$$

On the hub surface ($r = r_{\text{hub}}$), $p_2 = p_{2,\text{hub}}$ is fulfilled and therefore

$$c_{2\text{u,hub}} = u_{\text{hub}}\left(1 - \frac{n_{\text{N}}}{n}\frac{\dot{Q}}{\dot{Q}_{\text{N}}}\right) \tag{29}$$

Finally, one obtains

$$p_2 - p_{2,\text{hub}} = \frac{\rho}{2}\left(1 - \frac{n_{\text{N}}^2}{n^2}\frac{\dot{Q}^2}{\dot{Q}_{\text{N}}^2}\right)\left(u^2 - u_{\text{hub}}^2\right) \tag{30}$$

Because of $u = 2\pi nr$, the above equation represents a parabolic distribution of the static pressure at the runner exit.

At this moment, it appears to be interesting to discuss the relation between the pressure distribution according Eq. (30) and the velocity distribution $c_{2\mathrm{u}}$ according to Eq. (21). The flow at the runner exit must fulfil the Euler motion equation in the cylindrical coordinate system. For radial velocity component and with *z* as the axial coordinate, the Euler equation is expressed as

$$-\frac{1}{\rho}\frac{\partial p_2}{\partial r}=c_{2\mathrm{r}}\frac{\partial c_{2\mathrm{r}}}{\partial r}+c_{2\mathrm{z}}\frac{\partial c_{2\mathrm{r}}}{\partial z}-\frac{c_{2\mathrm{u}}^2}{r} \tag{31}$$

By applying the continuity equation, the first two terms on the r.h.s of the equation can be reformed, so that one obtains with $c_{2\mathrm{z}}=c_{2\mathrm{m}}$ and its uniform distribution:

$$\frac{1}{\rho}\frac{\partial p_2}{\partial r}=\frac{c_{2\mathrm{u}}^2}{r}+c_{2\mathrm{r}}^2\left[\frac{1}{r}+\frac{\partial}{\partial z}\left(\frac{c_{2\mathrm{m}}}{c_{2\mathrm{r}}}\right)\right] \tag{32}$$

The last term is denoted as *X*. With respect to Eq. (21) for $c_{2\mathrm{u}}$, one obtains through integration

$$p_2-p_{2,\mathrm{hub}}=\frac{\rho}{2}\left(1-\frac{n_\mathrm{N}}{n}\frac{\dot{Q}}{\dot{Q}_\mathrm{N}}\right)^2\left(u^2-u_{\mathrm{hub}}^2\right)+\rho\int_{r_\mathrm{hub}}^{r}X\mathrm{d}r \tag{33}$$

When compared with Eq. (30), it is evident that the last term in the above equation does not disappear. This indicates that in the cross-section at the runner exit the radial velocity component is nonzero. The flow is found in further development in the downstream flow. In fact, such a flow development has already started within the runner.

The further expansion of the flow causes the pressure redistribution. This will last until the integral term in Eq. (33) vanishes. In the duration, the circumferential velocity component and its distribution, however, remain constant because of the law of conservation of the angular momentum. This would be true only, if the flow section $A=\pi\left(R^2-r_{\mathrm{hub}}^2\right)$ would remain constant. The final pressure distribution, assumed in the fictitious downstream cross-section 3, is then computed from Eq. (30) and (33) as

$$\frac{p_3-p_{3,\mathrm{hub}}}{p_2-p_{2,\mathrm{hub}}}=\left(1+\frac{n_\mathrm{N}}{n}\frac{\dot{Q}}{\dot{Q}_\mathrm{N}}\right)\Big/\left(1-\frac{n_\mathrm{N}}{n}\frac{\dot{Q}}{\dot{Q}_\mathrm{N}}\right) \tag{34}$$

In the current paper, this pressure distribution is not further considered.

1.3 Euler Equation and Specific Work

The Euler equation for specific work basically represents the law of conservation for the angular momentum and specifies, in its given form, the energy exchange between the fluid flow and the runner of the Kaplan turbine. The specific work conducted by a unit mass is given by

$$Y = u_1 c_{1\mathrm{u}} - u_2 c_{2\mathrm{u}} \tag{35}$$

With respect to Eq. (11) for $c_{1\mathrm{u}}$ as well as with $u_1 = 2\pi rn$ and $\dot{Q} = \pi\left(R^2 - r_{\mathrm{hub}}^2\right)c_{\mathrm{m}}$, one obtains

$$u_1 c_{1\mathrm{u}} = 2\pi rn \frac{1}{r} \frac{c_{\mathrm{m}}}{\tan\alpha_0} \frac{R^2}{2b}\left(1 - \frac{r_{\mathrm{hub}}^2}{R^2}\right) = \frac{\dot{Q}}{\tan\alpha_0} \frac{n}{b} \tag{36}$$

The term $u_2 c_{2\mathrm{u}}$ in Eq. (35) is, according to Eq. (21), basically a function of the radial coordinate *r*. It disappears only under the nominal operating condition. Thus, for determining the overall averaged specific work, the mean value $\overline{u_2 c_{2\mathrm{u}}}$ must be obtained through integration. With the assumed uniform distribution of the meridian velocity component, the integration is simply performed as

$$\overline{uc_{2\mathrm{u}}} = \frac{1}{A}\int_{r_{\mathrm{hub}}}^{R} uc_{2\mathrm{u}} 2\pi r \mathrm{d}r = \frac{(\pi dn)^2}{2}\left(1 + \frac{r_{\mathrm{hub}}^2}{R^2}\right)\left(1 - \frac{n_{\mathrm{N}}}{n}\frac{\dot{Q}}{\dot{Q}_{\mathrm{N}}}\right) \tag{37}$$

The overall averaged specific work conducted in a Kaplan turbine then becomes

$$\overline{Y} = \frac{\dot{Q}}{\tan\alpha_0}\frac{n}{b} - \frac{(\pi dn)^2}{2}\left(1 + \frac{r_{\mathrm{hub}}^2}{R^2}\right)\left(1 - \frac{n_{\mathrm{N}}}{n}\frac{\dot{Q}}{\dot{Q}_{\mathrm{N}}}\right) \tag{38}$$

1.4 Hydraulic Efficiency

The effective pressure head (*H*) is commonly considered as the head between the section at the turbine inlet and the lower reservoir. This implies that the draft tube always belongs to the unit of a Kaplan turbine. The hydraulic efficiency of the turbine unit, thus, also accounts for the loss in the draft tube.

The specific work and the effective head are connected by the hydraulic efficiency in form $Y = \eta_{\mathrm{hyd}} gH$. For $Y = \overline{Y}$ with $\overline{Y}$ from Eq. (38), one obtains

$$\eta_{\mathrm{hyd}} = \frac{1}{b\tan\alpha_0}\frac{n\dot{Q}}{gH} - \frac{(\pi dn)^2}{2gH}\left(1 + \frac{r_{\mathrm{hub}}^2}{R^2}\right)\left(1 - \frac{n_{\mathrm{N}}}{n}\frac{\dot{Q}}{\dot{Q}_{\mathrm{N}}}\right) \tag{39}$$

With respect to unit parameters defined in Eq. (1) and because of $\dot{Q} = \pi\left(R^2 - r_{\mathrm{hub}}^2\right)c_{\mathrm{m}}$, it then follows from above equation

$$\eta_{\mathrm{hyd}} = \frac{2d}{\pi b}\frac{n_{11}\dot{Q}_{11}}{\tan\alpha_0} - \left(1 + \frac{r_{\mathrm{hub}}^2}{R^2}\right)\left(1 - \frac{n_{11,\mathrm{N}}}{n_{11}}\frac{\dot{Q}_{11}}{\dot{Q}_{11,\mathrm{N}}}\right)n_{11}^2 \tag{40}$$

This equation is denoted the *first energy equation* in hydromechanics of the Kaplan turbine, see Fig. 1. Its combined application with the *second energy equation*, as will be shown below in Sect. 1.7, leads to establishment of the *master equation* of the Kaplan turbine. Especially for $\eta_{\text{hyd}} = 0$, the so-called runaway speed of the Kaplan turbine can be obtained, see Sect. 3 below.

Under the nominal operating condition, the last term in above equation and Eq. (39) disappears. It then follows

$$\eta_{\text{hyd,N}} = \frac{2d}{\pi b} \frac{n_{11,\text{N}} \dot{Q}_{11,\text{N}}}{\tan \alpha_{0,\text{N}}} = \frac{1}{b} \frac{1}{\tan \alpha_{0,\text{N}}} \frac{n_{\text{N}} \dot{Q}_{\text{N}}}{gH} \tag{41}$$

This equation also reveals that the nominal discharge is simply determined by the geometrical configuration of the Kaplan turbine and the rotational speed. The hydraulic efficiency can be assumed, for instance, to be $\eta_{\text{hyd,N}} = 0.9$. It essentially depends on the draft tube design (opening to the tailwater).

1.5 Design Equations and Design Parameter

Each Kaplan turbine is designed for a specified nominal operating condition, under which the maximum efficiency of, say, $\eta_{\text{hyd,N}} = 0.9$, for instance, should be achieved. The remaining efficiency loss is mainly ascribed to the viscous friction and to the dissipated kinetic energy at the exit of the draft tube. From Eq. (41), one obtains

$$b \tan \alpha_{0,\text{N}} = \frac{1}{\eta_{\text{hyd,N}}} \frac{n_{\text{N}} \dot{Q}_{\text{N}}}{gH} = \frac{n_{\text{N}} \dot{Q}_{\text{N}}}{Y_{\text{N}}} \tag{42}$$

This equation is denoted as the *first design equation* of the Kaplan turbine. It directly relates the geometrical design of the wicket gate of a Kaplan turbine with nominal hydraulic parameters (H, $\dot{Q}_{\text{N}}$) and the rated rotational speed n_{N}. The nominal hydraulic efficiency $\eta_{\text{hyd,N}}$, in effect, behaves as being given. From *b*, if determined from above equation, then the runner diameter *d* can be estimated, commonly, with b/d=0.3−0.4. It should be noted that up to now the wicket gate height *b* has always been determined in reverse order, i.e., from the runner diameter *d* by b=(0.3−0.4)d, see [3, 4], without connecting with the guide-vane angle $\alpha_{0,\text{N}}$. This has the consequence that the above equation has been mostly not fulfilled.

In the present context of the *first design equation* given above, Eq. (15) together with Eq. (17) can be denoted as the *second design equation* and further Eq. (20) as the *third design* *equation* of the Kaplan turbine. Equation (17), which was given provisionally in Sect. 1.2.1, is obtained from Eqs. (16) and (42) by assuming $\eta_{\text{hyd,N}} = 1$.

With respect to Eqs. (3) and (4), the above equation can also be represented as a function of the nominal discharge and head coefficients.

According to Eq. (42), the upstream geometrical design (wicket gate) of a Kaplan turbine is obviously determined by $n_{\text{N}}\dot{Q}_{\text{N}}/gH$ which is called *design parameter* and denoted as σ_{d}. It determines not only the geometrical form but also the size of the Kaplan turbine. The latter is related to the parameter *b*, because the *design parameter* has a dimension of length. In contrast, when using the specific speed (speed number) defined in Eq. (7), as so until now, the dimensioning of the Kaplan turbine conceptually relies on the Cordier diagram. This means a two-step approximation concept: from the speed number to the diameter number. The practice of dimensioning the Kaplan turbine, as explained at beginning of Sect. 1.2 in connection with Eq. (7), is the use of empirical diagrams for the head coefficient $\psi = \text{f}\left(n_{\text{q}}\right)$.

The design parameter $\sigma_{\text{d}} = n_{\text{N}}\dot{Q}_{\text{N}}/gH$, thus, appears to be more applicable than the specific speed. Kaplan turbines that have equal design parameters, should have identical geometrical design (form and size). The author therefore suggests improving the old design rules, which have relied on the use of the specific speed n_{q}, by considering the design parameter σ_{d}.

The nominal guide-vane angle $\alpha_{0,\text{N}}$ in Eq. (42) should basically be set with respect to the sensitivity of regulating the flow. This aspect will be revealed below in Sect. 2.5 based on computations of an example Kaplan turbine.

1.6 Rate of Angular Momentum and Torque

For the purpose of conducting further analyses in subsequent sections, the angular momenta of the flows at both the runner inlet and exit are considered. At the runner inlet, the quantity is obtained by regarding $c_{1\text{u}}r$ from Eq. (11)

$$\dot{L}_1 = \rho\int_0^{\dot{Q}} c_{1\text{u}} r \,\text{d}\dot{Q} = \rho\frac{1}{\tan\alpha_0}\frac{\dot{Q}^2}{2\pi b} \tag{43}$$

It is, as expected, equal to the rate of the angular momentum at the wicket gate (Eq. (8)).

At the runner exit, where the velocity distribution ($c_{2\text{u}}$) is non-uniform, the angular momentum must be computed through integration. In view of Eq. (21) for $c_{2\text{u}}$ and by following the same computational procedure that led to Eq. (37), one obtains

$$\dot{L}_2=\rho\int_0^{\dot{Q}} c_{2u} r\mathrm{d}\dot{Q}=\pi\left(R^2+r_{\mathrm{hub}}^2\right)\left(1-\frac{n_{\mathrm{N}}}{n}\frac{\dot{Q}}{\dot{Q}_{\mathrm{N}}}\right)n\rho\dot{Q} \tag{44}$$

The hydraulic torque is determined by the difference between the two rates of angular momentum ($\dot{L}_1$ and $\dot{L}_2$), as given in the following form:

$$M_{\mathrm{hyd}}=\dot{L}_1-\dot{L}_2=\frac{\rho}{\tan\alpha_0}\frac{\dot{Q}^2}{2\pi b}-\pi\left(R^2+r_{\mathrm{hub}}^2\right)\left(1-\frac{n_{\mathrm{N}}}{n}\frac{\dot{Q}}{\dot{Q}_{\mathrm{N}}}\right)n\rho\dot{Q} \tag{45}$$

With respect to Eq. (1), it is further written as

$$M_{11}=\frac{1}{\tan\alpha_0}\frac{d}{\pi b}\dot{Q}_{11}^2-\frac{1}{2}\left(1+\frac{r_{\mathrm{hub}}^2}{R^2}\right)\left(1-\frac{n_{11,\mathrm{N}}}{n_{11}}\frac{\dot{Q}_{11}}{\dot{Q}_{11,\mathrm{N}}}\right)n_{11}\dot{Q}_{11} \tag{46}$$

As will be shown later, this equation can be used to compute the runaway speed by setting $M_{11}=0$.

1.7 Examination of Existing Losses

The hydraulic efficiency of a Kaplan turbine can be computed if all hydraulic losses are known. Basically, all possible hydraulic losses can be categorised into the flow-dependent friction-dominant losses and the losses which only occur when the turbine operates at off-design points. The latter includes the shock loss at the runner inlet and the swirling loss at the runner exit. It is of the same concept as at the Francis turbine [2]. Thus, the hydraulic efficiency of a Kaplan turbine can be expressed as

$$\eta_{\mathrm{hyd}}=1-\Delta\eta_{\mathrm{Q}}-\Delta\eta_{\mathrm{shock}}-\Delta\eta_{\mathrm{swirl}} \tag{47}$$

Other types of losses can be thought to be included in $\Delta\eta_{\mathrm{Q}}$. The respective losses in above equation are considered below in details.

Equation (47) is denoted as the *second energy equation* in hydromechanics of the Kaplan turbine, see Fig. 1. Together with the first energy equation, i.e., Eq. (40), the master equation can be derived (Sect. 2 below).

1.7.1 Flow-Related Friction-Dominant Losses

The friction losses are mainly found in the wicket gate, in the runner, and in the draft tube. They are all proportional to the square of the discharge. Other similar losses are related partially to the mixing and redistribution of the flow downstream of the runner and partially to the dissipation of the kinetic energy of the flow out of the draft tube into the lower reservoir. For simplicity, all these losses are assumed to be proportional to the square of discharge. With the cross-sectional area of the flow at the runner (A) as reference, the sum of frictional and flow-related internal losses is, then, represented as

$$\Delta \eta_{\mathrm{Q}} = \zeta_{\mathrm{Q}} \frac{1}{2gH} \left(\frac{\dot{Q}}{A} \right)^2 \tag{48}$$

Here, ζ_{Q} is the head drop coefficient.

With respect to the definition of unit discharge according to Eq. (1) and because of $A = \pi \left(R^2 - r_{\mathrm{hub}}^2 \right)$, the above equation is also written as

$$\Delta \eta_{\mathrm{Q}} = \frac{\zeta_{\mathrm{Q}}}{\left(1 - r_{\mathrm{hub}}^2 / R^2 \right)^2} \frac{16}{\pi^2} \dot{Q}_{11}^2 \tag{49}$$

The pressure drop coefficient ζ_{Q} can be determined from the nominal operation point, at which the hydraulic efficiency, for instance, is known as $\eta_{\mathrm{hyd,N}} = 0.9$. Then from Eq. (41), the nominal discharge $\dot{Q}_{\mathrm{N}}$ or $\dot{Q}_{11,\mathrm{N}}$ is computed. Finally, one obtains the pressure drop coefficient ζ_{Q} from Eq. (48) or Eq. (49) with $\Delta \eta_{\mathrm{Q,N}} = 1 - \eta_{\mathrm{hyd,N}} = 0.1$.

1.7.2 Shock Loss at the Runner Inlet

The shock loss is related to the flow at the runner inlet and occurs at off-design points of the Kaplan turbine. It arises from the abrupt change in the direction of the flow and so from the flow separation along the leading edge of each runner blade and subsequent redistribution of the flow within the blade channels. The mechanism of leading to hydraulic loss is the same, as the Borda–Carnot shock loss relies on.

According to Fig. 4, in which the velocity triangle is shown for a partial load, the shock loss in form of the head drop is given by

$$\Delta h_{\mathrm{shock}} = \mu_{\mathrm{sh}} \frac{(\Delta w_1)^2}{2g} \tag{50}$$

The coefficient μ_{sh} accounts for the part of the shock loss at the theoretical maximum.

Then, the shock loss is expressed in term of efficiency loss as $\Delta \eta_{\mathrm{shock}} = \Delta h_{\mathrm{shock}} / H$. Based on the geometrical relation presented in Fig. 4 and by applying the relative velocity w_1, the shock loss is further expressed as

$$\Delta \eta_{\mathrm{shock}} = \mu_{\mathrm{sh}} \frac{\sin^2 (\beta_1 - \beta_{1\mathrm{b}})}{\sin^2 \beta_{1\mathrm{b}}} \frac{w_1^2}{2gH} = \mu_{\mathrm{sh}} \left(\frac{1}{\tan \beta_{1\mathrm{b}}} - \frac{1}{\tan \beta_1} \right)^2 \frac{c_{\mathrm{m}}^2}{2gH} \tag{51}$$

Here, β_{1b} represents the design angle of runner blades on their leading edge. Only when the flow angle β_1 equals the blade angle β_{1b}, the shock loss vanishes.

In using of the definition of unit discharge $\dot{Q}_{11}$, the meridian velocity c_m is further expressible as

$$\frac{c_m^2}{2gH}=\frac{16\dot{Q}_{11}^2}{\pi^2\left(1-r_{hub}^2/R^2\right)^2} \tag{52}$$

Substituting this equation into Eq. (51) yields

$$\Delta\eta_{shock}=\mu_{sh}\left(\frac{1}{\tan\beta_{1b}}-\frac{1}{\tan\beta_1}\right)^2\frac{16\dot{Q}_{11}^2}{\pi^2\left(1-r_{hub}^2/R^2\right)^2} \tag{53}$$

For $\tan\beta_1$ and $\tan\beta_{1b}$ in above equation, one obtains from Eq. (14) with respect to β_{1b} for nominal operation

$$\frac{1}{\tan\beta_{1b}}-\frac{1}{\tan\beta_1}=R^2\left[\frac{2\pi r}{d^3}\left(\frac{n_{11,N}}{\dot{Q}_{11,N}}-\frac{n_{11}}{\dot{Q}_{11}}\right)-\frac{1}{2br}\left(\frac{1}{\tan\alpha_{0,N}}-\frac{1}{\tan\alpha_0}\right)\right]\left(1-\frac{r_{hub}^2}{R^2}\right) \tag{54}$$

Thus, the shock loss is further written as

$$\Delta\eta_{shock}=\frac{\mu_{sh}}{\pi^2}\left[\frac{2\pi r}{d}\left(\frac{n_{11,N}}{\dot{Q}_{11,N}}-\frac{n_{11}}{\dot{Q}_{11}}\right)-\frac{d^2}{2br}\left(\frac{1}{\tan\alpha_{0,N}}-\frac{1}{\tan\alpha_0}\right)\right]^2\dot{Q}_{11}^2 \tag{55}$$

The shock loss is directly related to the control parameter α_0, but is still a function of the radial coordinate. Its mean value is obtained by the integration

$$\overline{\Delta\eta_{shock}}=\frac{1}{\dot{Q}}\int_{r_{hub}}^{R}\Delta\eta_{shock}2\pi r c_m \mathrm{d}r \tag{56}$$

This leads to

$$\begin{aligned}\frac{\overline{\Delta\eta_{shock}}}{\mu_{sh}\dot{Q}_{11}^2}=&\frac{1}{2}\left(1+\frac{r_{hub}^2}{R^2}\right)\left(\frac{n_{11,N}}{\dot{Q}_{11,N}}-\frac{n_{11}}{\dot{Q}_{11}}\right)^2\\&-\frac{2d}{\pi b}\left(\frac{n_{11,N}}{\dot{Q}_{11,N}}-\frac{n_{11}}{\dot{Q}_{11}}\right)\left(\frac{1}{\tan\alpha_{0,N}}-\frac{1}{\tan\alpha_0}\right)\\&+\frac{2d^2}{(\pi b)^2}\left(\frac{1}{\tan\alpha_{0,N}}-\frac{1}{\tan\alpha_0}\right)^2\frac{\ln\left(R/r_{hub}\right)}{1-r_{hub}^2/R^2}\end{aligned} \tag{57}$$

Except for $\dot{Q}_{11}$ and n_{11}, all other parameters in this equation are referred to either the nominal operation or geometrical specifications. They can, thus, be considered as given.

Equation (57) will be used in connection with the swirling loss at the runner exit to compute the main loss in the Kaplan turbine for both the partial load and the overload.

1.7.3 Swirling Loss at the Runner Exit

In this section, only the runner with fixed blades is considered.

At partial load or overload, the exit flow out of the runner possesses a circumferential velocity component, see Eq. (21). The kinetic energy contained in this swirling flow will be dissipated in the downstream draft tube and thus should be basically considered as being lost.

Because of the non-uniform distribution of the circumferential velocity component c_{2u}, as given in Eq. (21), the averaged mean of the kinetic energy is obtained through integration. This is given as

$$\frac{1}{2}\overline{c_{2u}^2} = \frac{(2\pi n)^2}{2}\left(1-\frac{n_N}{n}\frac{\dot{Q}}{\dot{Q}_N}\right)^2 \frac{1}{\dot{Q}}\int_{r_{hub}}^{R} r^2 2\pi r c_m \mathrm{d}r \tag{58}$$

By assuming the uniform axial velocity component c_m, one obtains

$$\frac{1}{2}\overline{c_{2u}^2} = \frac{(\pi d n)^2}{4}\left(1+\frac{r_{hub}^2}{R^2}\right)\left(1-\frac{n_N}{n}\frac{\dot{Q}}{\dot{Q}_N}\right)^2 \tag{59}$$

The corresponding efficiency loss is further computed. Using the unit parameters defined in Eq. (1) follows

$$\Delta\eta_{swirl} = \frac{1}{2gH}\overline{c_{2u}^2} = \frac{1}{2}\left(1+\frac{r_{hub}^2}{R^2}\right)\left(\frac{n_{11}}{n_{11,N}}-\frac{\dot{Q}_{11}}{\dot{Q}_{11,N}}\right)^2 n_{11,N}^2 \tag{60}$$

It is worth noting that between Eqs. (37) and (59) the following relation can be found:

$$\frac{\frac{1}{2}\overline{c_{2u}^2}}{\overline{\overline{uc_{2u}}}} = \frac{1}{2}\left(1-\frac{n_N}{n}\frac{\dot{Q}}{\dot{Q}_N}\right), \tag{61}$$

which is similar to that at the Francis turbine [2].

2 Master Equation of the Kaplan Turbine

The first and second energy equations have been derived in Eqs. (40) and (47), respectively. To Eq. (47), corresponding terms have also been worked out in detail. In this section, as indicated in Fig. 1, the master equation of the Kaplan turbine will be presented.

2.1 Discharge

Combining Eqs. (40) and (47) to collect all partial losses, one obtains, after proper rearrangement

$$k_\mathrm{A}\dot{Q}_{11}^2+k_\mathrm{B}\dot{Q}_{11}+k_\mathrm{C}=0 \tag{62}$$

with

$$k_\mathrm{A}=\frac{1+\mu_\mathrm{sh}}{2}\left(1+\frac{r_\mathrm{hub}^2}{R^2}\right)\frac{n_{11,\mathrm{N}}^2}{\dot{Q}_{11,\mathrm{N}}^2}+\frac{16}{\pi^2}\frac{\zeta_\mathrm{Q}}{\left(1-r_\mathrm{hub}^2/R^2\right)^2}$$

$$-\mu_\mathrm{sh}\frac{2d}{\pi b}\left(\frac{1}{\tan\alpha_{0,\mathrm{N}}}-\frac{1}{\tan\alpha_0}\right)\frac{n_{11,\mathrm{N}}}{\dot{Q}_{11,\mathrm{N}}}+\frac{\mu_\mathrm{sh}}{2}\left(\frac{2d}{\pi b}\right)^2\left(\frac{1}{\tan\alpha_{0,\mathrm{N}}}-\frac{1}{\tan\alpha_0}\right)^2\frac{\ln\left(R/r_\mathrm{hub}\right)}{1-r_\mathrm{hub}^2/R^2}$$

$$k_\mathrm{B}=\frac{2d}{\pi b}\left(\frac{\mu_\mathrm{sh}}{\tan\alpha_{0,\mathrm{N}}}+\frac{1-\mu_\mathrm{sh}}{\tan\alpha_0}\right)n_{11}-\mu_\mathrm{sh}\left(1+\frac{r_\mathrm{hub}^2}{R^2}\right)\frac{n_{11,\mathrm{N}}}{\dot{Q}_{11,\mathrm{N}}}n_{11}$$

$$k_\mathrm{C}=-\frac{1}{2}\left(1-\mu_\mathrm{sh}\right)\left(1+\frac{r_\mathrm{hub}^2}{R^2}\right)n_{11}^2-1$$

This equation is called the *master equation of the Kaplan turbine*. It is a simple quadratic polynomial for the unit discharge $\dot{Q}_{11}$, comparable to the master equation of the Francis turbine [2]. All three coefficients are simply a function of the rotational speed n_{11} and the guide-vane angle α_0. Because other parameters are either geometrical parameters or parameters related to the nominal operating point, the master equation basically represents a function of $\dot{Q}_{11}=\mathrm{f}\left(\alpha_0,n_{11}\right)$, with α_0 as the regulation or control parameter.

The expressions of all three coefficients appear to be somewhat complex. This is because they all account for the outcomes of viscous friction effect, shock and swirling losses, which are of different fluid mechanics. For approximation, $\mu_\mathrm{sh}\approx 1$ is applicable. Then, both the coefficients k_B and k_C can be considerably simplified. The assumption of $\zeta_\mathrm{Q}=0$, however, is basically not admissible, because at the Kaplan turbine the volume flow rate is commonly high and so is the resultant loss. The author would like to emphasize that no any other mathematical approximations should be made, because the master equation exactly represents a closed solution of the Kaplan turbine and thus always provides reasonable computational results.

The expression $n_{11,\mathrm{N}}/\dot{Q}_{11,\mathrm{N}}$ in both coefficients k_A and k_B can be replaced by the nominal discharge coefficient φ_N according to Eq. (6).

The nominal discharge is obtained under the nominal guide-vane opening $\alpha_{0,\mathrm{N}}$ directly from Eq. (41) with $\eta_\mathrm{hyd,N}=0.9$, for instance. When the master equation is applied, the computation finally leads to Eq. (41) as well.

At $n_{11}=0$, it is about a free-flow process through the Kaplan turbine. The unit discharge is obtained in this case as

$$\dot{Q}_{11,\mathrm{n=0}}=\frac{1}{\sqrt{k_{\mathrm{A}}}}. \tag{63}$$

Because of the composition of the coefficient k_{A}, the discharge at $n=0$ is primarily determined by the shock loss at the runner inlet and the swirling flow at the runner exit. The discharge will be considerably reduced, see also the computational example below in Sect. 2.5.

At the nominal setting of guide vanes ($\alpha_{0,\mathrm{N}}$) and by neglecting the friction-dominant losses ($\zeta_{\mathrm{Q}}\approx 0$) as well as with $\mu_{\mathrm{sh}}\approx 1$, the coefficient k_{A} is simplified to

$$k_{\mathrm{A,N}}\approx\left(1+\frac{r_{\mathrm{hub}}^2}{R^2}\right)\frac{n_{11,\mathrm{N}}^2}{\dot{Q}_{11,\mathrm{N}}^2} \tag{64}$$

With respect to both $\dot{Q}_{11,\mathrm{N}}$ according to Eq. (1) and $\psi_{\mathrm{N}}=1/n_{11,\mathrm{N}}^2$ according to Eq. (4), the ratio of the free flow through the Kaplan turbine to the nominal discharge is obtained from Eq. (63)

$$\frac{\dot{Q}_{\mathrm{n=0,N}}}{\dot{Q}_{\mathrm{N}}}\approx\left(\frac{\psi_{\mathrm{N}}}{1+r_{\mathrm{hub}}^2/R^2}\right)^{0.5} \tag{65}$$

For $\psi_{\mathrm{N}}=0.3$ and $r_{\mathrm{hub}}/R=0.43$, for instance, one obtains $\dot{Q}_{\mathrm{n=0,N}}/\dot{Q}_{\mathrm{N}}\approx 0.5$, corresponding to a reduction in discharge by a factor 2. This is the reason, why in Eq. (64) the approximation of $\zeta_{\mathrm{Q}}\approx 0$ has been applied.

On the other hand, the unit discharge given in Eq. (63) can also be directly obtained from Eq. (57) for shock loss, from Eq. (60) for swirling loss and from Eq. (49) for flow-dependent friction loss by setting $n_{11}=0$ and subsequently using $\Delta\eta_{\mathrm{shock,0}}+\Delta\eta_{\mathrm{swirl,0}}+\Delta\eta_{\mathrm{Q}}=1$. Thus, the free discharge at $n_{11}=0$ is completely governed by shock, swirling, and friction losses. The last factor is, as just shown above, mostly negligible.

2.2 Hydraulic Efficiency

The hydraulic efficiency of a Kaplan turbine is given, once the discharge has been computed from Eq. (62) and subsequently inserted into Eq. (40). In the practice, it has often been shown in form of a hill chart. The related computations will be presented below in Sect. 2.5 in association with a computation example.

2.3 Hydraulic Torque and Power

Accounting for the hydraulic efficiency, the hydraulic power of a Kaplan turbine is computed as

$$P_{\text{hyd}} = \eta_{\text{hyd}} \rho g H \dot{Q} \tag{66}$$

The computation of the hydraulic efficiency is referred to Eq. (40) or, equivalently, to Eq. (47).

On the other hand, the hydraulic power is represented as the product of the hydraulic torque exerted on the shaft (moment M_{hyd}) and the angular speed ($2\pi n$) of the shaft, as given by $P_{\text{hyd}} = 2\pi n M_{\text{hyd}}$. By equalising this equation with Eq. (66) and further by applying Eq. (1), one obtains

$$M_{11} = \frac{\eta_{\text{hyd}}}{2} \frac{\dot{Q}_{11}}{n_{11}} \tag{67}$$

In this equation, the unit discharge $\dot{Q}_{11} = \mathrm{f}\left(n_{11}, \alpha_0\right)$ has already been computed by the master equation, viz. Eq. (62).

Furthermore, from Eq. (2) the power coefficient λ_{11} is also obtainable.

Equation (67) in its given form could not be directly applied to the case $n = 0$. From Eq. (46), however, one obtains immediately

$$M_{11,\text{n=0}} = \left[\frac{1}{\tan\alpha_0} \frac{d}{\pi b} + \frac{1}{2}\left(1 + \frac{r_{\text{hub}}^2}{R^2}\right) \frac{n_{11,\text{N}}}{\dot{Q}_{11,\text{N}}} \right] \dot{Q}_{11,\text{n=0}}^2 \tag{68}$$

For $\dot{Q}_{11,\text{n=0}}$ refer to Eq. (63).

For nominal setting of guide vanes ($\alpha_{0,\text{N}}$) and in applying Eq. (67), one obtains the ratio of the torque to the nominal torque under the nominal operating condition:

$$\frac{M_{11,\text{n=0,N}}}{M_{11,\text{N}}} = \frac{2\dot{Q}_{11,\text{n=0,N}}^2 n_{11,\text{N}}}{\eta_{\text{hyd,N}} \dot{Q}_{11,\text{N}}} \left[\frac{1}{\tan\alpha_{0,\text{N}}} \frac{d}{\pi b} + \frac{1}{2}\left(1 + \frac{r_{\text{hub}}^2}{R^2}\right) \frac{n_{11,\text{N}}}{\dot{Q}_{11,\text{N}}} \right] \tag{69}$$

The term $\tan\alpha_{0,\text{N}}$ is substituted by Eq. (41), yields

$$\frac{M_{11,\text{n=0,N}}}{M_{11,\text{N}}} = \left[\frac{1}{n_{11,\text{N}}^2} + \left(1 + \frac{r_{\text{hub}}^2}{R^2}\right) \frac{1}{\eta_{\text{hyd,N}}} \right] \frac{\dot{Q}_{11,\text{n=0,N}}^2}{\dot{Q}_{11,\text{N}}^2} n_{11,\text{N}}^2 \tag{70}$$

When using respective physical quantities ($M_{\text{hyd,N}}$ and $\dot{Q}_{\text{N}}$) and the approximation of Eq. (65), one obtains with further consideration of $n_{11,\text{N}}^2 = 1/\psi_{\text{N}}$

$$\frac{M_{\text{hyd,n=0,N}}}{M_{\text{hyd,N}}} \approx \frac{\psi_{\text{N}}}{1+r_{\text{hub}}^2/R^2} + \frac{1}{\eta_{\text{hyd,N}}} \tag{71}$$

It is a function of the geometric design of the Kaplan turbine.

2.4 Reconstruction of the Master Equation

The master equation in the given form at Eq. (62) is suitable to compute characteristics of the Kaplan turbine in the basic form of discharge $\dot{Q}_{11} = \text{f}\left(n_{11}, \alpha_0\right)$ and subsequently also of other operation parameters like efficiency η_{hyd} and power coefficient λ_{11}. Computation examples will be shown in Sect. 2.5. Sometimes, as for special applications, the master equation needs to be reformed. This has been demonstrated to be much helpful at the Francis turbine, when hydraulic transients in a hydraulic system with Francis turbines should be computed [13].

For extended applications, therefore, the master equation given at Eq. (62) is reformed to

$$m_2\dot{Q}_{11}^2 + m_1\left(n_{11}\dot{Q}_{11}\right) + m_0 n_{11}^2 - 1 = 0 \tag{72}$$

The corresponding coefficients m_2, m_1 and m_0 can be obtained from the coefficients k_{A}, k_{B} and k_{C} as follows:

$$m_2 = k_{\text{A}}$$

$$m_1 = k_{\text{B}}/n_{11}$$

$$m_0 = \frac{k_{\text{C}}+1}{n_{11}^2} = -\frac{1}{2}\left(1-\mu_{\text{sh}}\right)\left(1+\frac{r_{\text{hub}}^2}{R^2}\right)$$

All these three coefficients do not contain the unit speed n_{11}. Especially for $\mu_{\text{sh}} \approx 1$ there is $m_0 = 0$. Correspondingly, the coefficient m_1 is simplified to

$$m_1 = \frac{k_{\text{B}}}{n_{11}} = \frac{2d}{\pi b}\frac{1}{\tan\alpha_{0,\text{N}}} - \left(1+\frac{r_{\text{hub}}^2}{R^2}\right)\frac{n_{11,\text{N}}}{\dot{Q}_{11,\text{N}}} \tag{73}$$

It is even independent of the control parameter α_0 of guide vanes at the wicket gate.

The *reconstructed master equation* has applications in computations of hydraulic transients which are caused, for instance, by starting, stopping, or regulating the turbine load in a hydraulic system with Kaplan turbines. Another application is the computation of the runaway speed of the Kaplan turbine, as will be shown below in Sect. 3.

2.5 Computational Example

The significance of the master equation is evidenced in analytical computations of complete hydraulic performances of a given Kaplan turbine. In order to show the applicability of the derived master equation, a virtually configured Kaplan turbine with the given dimensioning and the nominal operating condition (H, n) according to Table 1 is considered. The computations are rather for the plotting of hydraulic characteristics than for the geometric design. This is because with all given parameters the runner is supposed to be available for optimal performance, including the blade number and geometry. While the former is largely based on experiences, the latter exactly follows the second and third design equations, see Eqs. (15) and (20). Because of this, the nominal discharge behaves as a result of calculations rather than as prescribed. The assumed efficiency loss $\Delta\eta_{\mathrm{Q,N}} = 0.1$ already accounts for the hydraulic performance of the draft tube.

Table 1 A virtual Kaplan turbine with nominal parameters ($\mu_{\mathrm{sh}} = 1$)

Given parameters:	Unit	Value
Nominal head H	m	13
Nominal rotational speed n_{N}	rpm	200
Runner diameter d	m	2.8
Hub radius r_{hub}	m	0.6
Guide-vane opening $\alpha_{0,\mathrm{N}}$	deg.	45
Wicket gate height b	m	1.5
Efficiency loss $\Delta\eta_{\mathrm{Q,N}}$	-	0.1
Computed parameters:		
Hydraulic efficiency $\eta_{\mathrm{hyd,N}}$	-	0.90
Nominal discharge $\dot{Q}_{\mathrm{N}}$	m³/s	51.6
Head loss coefficient ζ_{Q}	-	0.242
Discharge coefficient φ_{N}	-	0.286
Head coefficient ψ_{N}	-	0.297
Hydraulic power P_{hyd}	MW	5.92
Specific speed n_{q}	-	210
Runaway speed $n_{11,\mathrm{R,N}}$	-	4.09
Runaway speed $n_{\mathrm{R,N}}$	rpm	445
Runaway discharge $\dot{Q}_{11,\mathrm{R,N}}$	-	0.75
Runaway discharge $\dot{Q}_{\mathrm{R,N}}$	m³/s	93.8

While the nominal discharge $\dot{Q}_{\mathrm{N}}$ is computed from Eq. (41), the pressure drop coefficient ζ_{Q} is determined from Eq. (48).

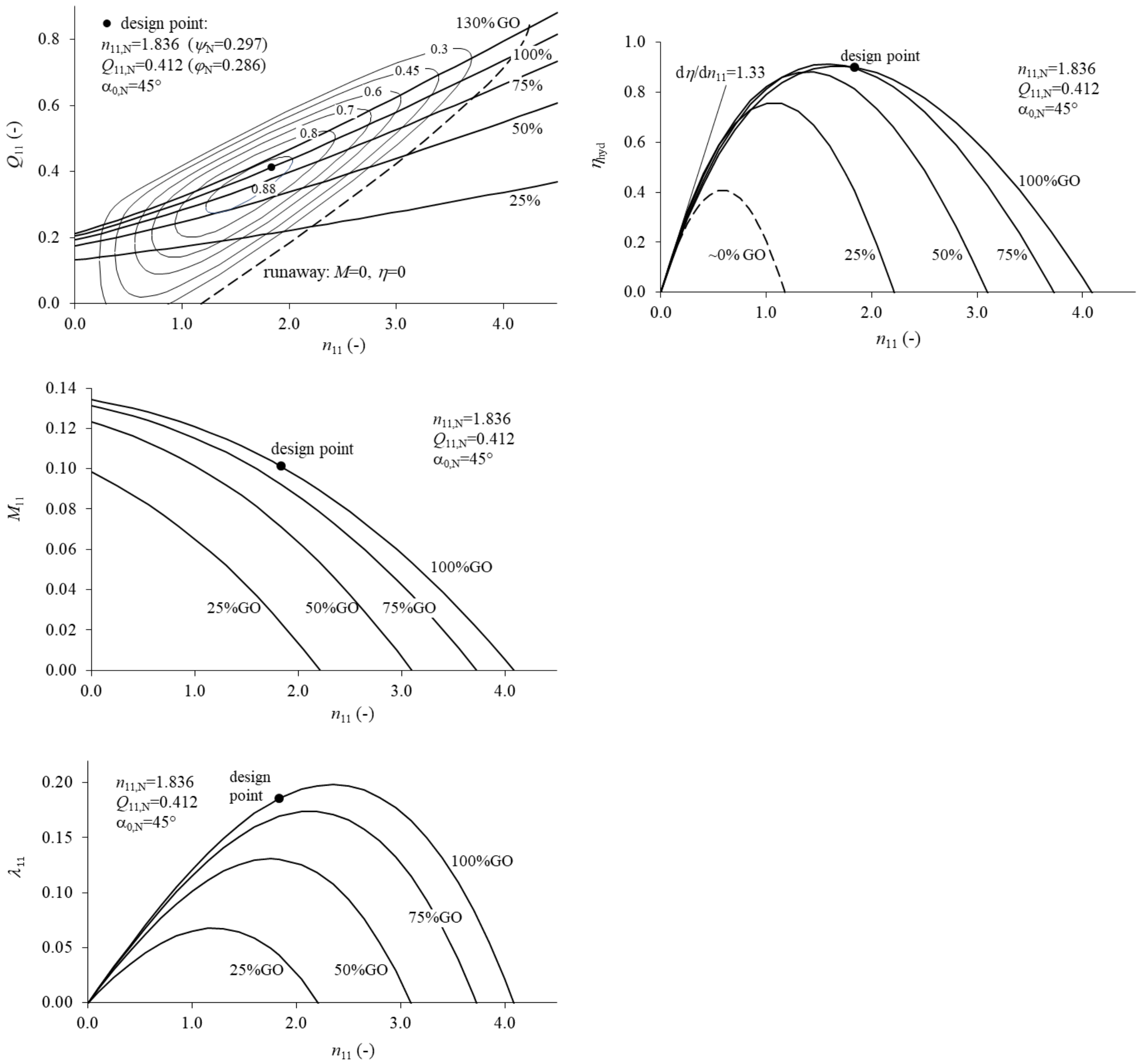

Fig. 5 Characteristics of the Kaplan turbine as functions of the unit speed and the guide-vane opening (GO), computed from the master eqution

Figure 5 shows computational results regarding unit discharge, unit momentum, hydraulic efficiency, and power coefficient. The efficiency hill chart has also been shown. Following remarkable points can be drawn:

- The sensitivity of load regulation is smaller at large guide-vane angles (α_0). This implies that for setting the nominal guide-vane opening, one should always carry out corresponding computations regarding the regulation sensitivity. After $\alpha_{0,\mathrm{N}}$ has been chosen, the *first design equation* (42) can be applied to size the Kaplan turbine by computing the parameter b. For better applications, both parameters should be optimized by combining them.

- From the diagram $\dot{Q}_{11}=\mathrm{f}\left(n_{11},\alpha_0\right)$, one reads out that for the nominal opening of guide vanes (100% GO) the ratio of the free flow through the turbine (n=0) to the nominal discharge is about 0.5. This accurately agrees with the value which is calculated from Eq. (65).
- From the diagram $M_{11}=\mathrm{f}\left(n_{11},\alpha_0\right)$, one reads out that again for the nominal opening of guide vanes (100% GO) the hydraulic torque at n=0 is about 1.33 times of the torque under the designed operating point. This agrees well with the computation of Eq. (71) leading to a torque ratio of 1.36.
- At the design point, the hydraulic efficiency measures 90%. It agrees with the given value in Table 1. One confirms that a small reduction of the unit number from the nominal value even leads to an increase in the efficiency. This is simply because of the dominant reduction of the friction-dependent loss $\Delta\eta_{\mathrm{Q}}$, while the increase of other two losses ($\Delta\eta_{\mathrm{shock}}$ and $\Delta\eta_{\mathrm{swirl}}$) are negligible. Therefore, the best efficiency point (BEP) of a Kaplan turbine, commonly and accurately, always slightly differs from the design point.
- At n=0, the gradient of the efficiency curve can be computed from Eq. (40) as

$$\left.\frac{\mathrm{d}\eta_{\mathrm{hyd}}}{\mathrm{d}n_{11}}\right|_{\mathrm{n=0}}=\left[\frac{2d}{\pi b}\frac{1}{\tan\alpha_0}+\left(1+\frac{r_{\mathrm{hub}}^2}{R^2}\right)\frac{n_{11,\mathrm{N}}}{\dot{Q}_{11,\mathrm{N}}}\right]\dot{Q}_{11,\mathrm{n=0}} \tag{74}$$

If compared with Eq. (68), one obtains

$$\left.\frac{\mathrm{d}\eta_{\mathrm{hyd}}}{\mathrm{d}n_{11}}\right|_{\mathrm{n=0}}=2\frac{M_{11,\mathrm{n=0}}}{\dot{Q}_{11,\mathrm{n=0}}} \tag{75}$$

It appears to be a logical result as from Eq. (67).

Further, the nominal setting of guide vanes is considered. In view of Eq. (41), the above equation becomes

$$\left.\frac{\mathrm{d}\eta_{\mathrm{hyd}}}{\mathrm{d}n_{11}}\right|_{\mathrm{n=0,N}}=\left[\frac{\eta_{\mathrm{hyd,N}}}{n_{11,\mathrm{N}}}+\left(1+\frac{r_{\mathrm{hub}}^2}{R^2}\right)n_{11,\mathrm{N}}\right]\frac{\dot{Q}_{11,\mathrm{n=0,N}}}{\dot{Q}_{11,\mathrm{N}}} \tag{76}$$

Then, with respect to Eq. (65) as an approximation and $\psi_{\mathrm{N}}=1/n_{11,\mathrm{N}}^2$, one finally obtains

$$\left.\frac{\mathrm{d}\eta_{\mathrm{hyd}}}{\mathrm{d}n_{11}}\right|_{\mathrm{n=0,N}}\approx\frac{\eta_{\mathrm{hyd,N}}\psi_{\mathrm{N}}}{\sqrt{1+r_{\mathrm{hub}}^2/R^2}}+\sqrt{1+\frac{r_{\mathrm{hub}}^2}{R^2}} \tag{77}$$

Basically, if $\zeta_{\mathrm{Q}}=0$ would be true rather than an approximation, then $\eta_{\mathrm{hyd,N}}=1$ should be applied.

In the current computational example, a gradient of $\left(\mathrm{d}\eta_{\mathrm{hyd}}/\mathrm{d}n_{11}\right)_{\mathrm{n=0,N}}=1.333$ is directly obtained from above equation, as shown in the diagram. It approximately also applies to other guide-vane settings. Especially, the above equation can be applied, for instance, to extrapolate measurements to n=0 and to create regression curves.

- For the curve of runaway (M=0) in diagram $\dot{Q}_{11}=\mathrm{f}\left(n_{11},\alpha_0\right)$, see Sect. 3 below.

The characteristics of the Kaplan turbine describe the turbine performances under the operating conditions out of the design point. The associated remarkable occurrences in the flow are the shock and swirling losses, as described in Sect. 1.7. In the computational example presented here, these two types of losses have also been computed, as shown in Fig. 6 for a guide-vane setting of $\alpha_0=30°$. It is obvious that both the shock and swirling losses dominate at both partial and overloads.

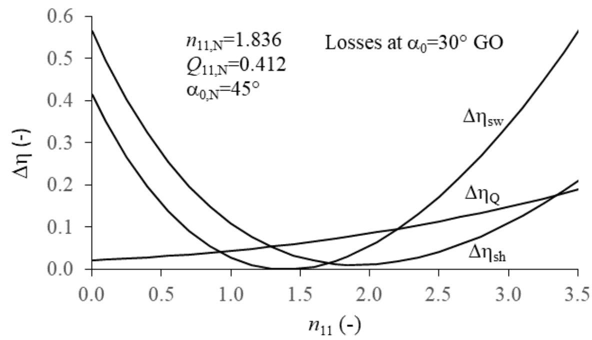

Fig. 6 Main losses in the considered Kaplan turbine at a partial load which is given by the guide-vane opening of α_0=30°

3 Runaway Speed of the Kaplan Turbine

A special case at the Kaplan turbine is the case of emergency load rejection for some reasons. The available head and the water flow then force the turbine unit to speed up towards a maximum which is called the *runaway speed*.

The maximum runaway speed behaves as a critical value for the mechanical safety of both the turbine runner and the rotor of the generator. Because under the runaway speed no energy exchange between the flow and the runner occurs, both the hydraulic efficiency and the torque vanish ($\eta_{\mathrm{hyd,R}}=0$ and $M_{11,\mathrm{R}}=0$). The runaway speed is thus a clearly defined parameter. In

Fig. 5, one confirms, for instance for $\eta_{\text{hyd,R}}=0$, quite different runaway speeds for different guide-vane openings.

From Eq. (40) or Eq. (46), one first obtains the ratio $n_{11,\text{R}}/\dot{Q}_{11,\text{R}}$ as

$$S(\alpha_0)=\frac{n_{11,\text{R}}}{\dot{Q}_{11,\text{R}}}=\frac{n_{11,\text{N}}}{\dot{Q}_{11,\text{N}}}+\frac{2d}{\pi b}\frac{1}{\tan\alpha_0}\frac{1}{1+r_{\text{hub}}^2/R^2} \tag{78}$$

as a function of guide-vane angle α_0. It is obviously of completely geometrical character.

On the other hand, one obtains from the reconstructed master equation, i.e., Eq. (72)

$$m_2\dot{Q}_{11,\text{R}}^2+m_1\left(n_{11,\text{R}}\dot{Q}_{11,\text{R}}\right)+m_0 n_{11,\text{R}}^2-1=0 \tag{79}$$

From Eqs. (78) and (79), both the unit runaway speed and the unit discharge are expressed as

$$n_{11,\text{R}}(\alpha_0)=\frac{1}{\sqrt{m_2/S^2+m_1/S+m_0}} \tag{80}$$

$$\dot{Q}_{11,\text{R}}(\alpha_0)=\frac{1}{\sqrt{m_2+m_1 S+m_0 S^2}} \tag{81}$$

The runaway speed and the associated discharge have been derived as a function of the guide-vane angle (α_0). The approximation $\mu_{\text{sh}}\approx 1$ and hence $m_0=0$ can be applied without causing any significant inaccuracies. Figure 7 shows corresponding computational results for the Kaplan turbine which has been considered in Fig. 5.

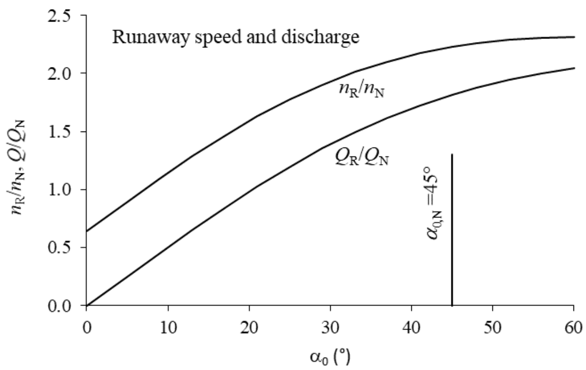

Fig. 7 Runaway speed and discharge of the considered Kaplan turbine

In the case that guide vanes tend to be closed ($\alpha_0\rightarrow 0$), there is $n_{\text{R}}\neq 0$. This is because according to the master equation, the angle α_0 can mathematically never be set to be zero. In addition, Eq. (40) with $\eta_{\text{hyd}}=0$ basically has two solutions, one is $n_{11}=0$ and another $n_{11}\neq 0$, see the η-curves in Fig. 5. While obtaining Eq. (78) from Eq. (40), the first solution $n_{11}=0$

has been erased. From Eq. (78) and (79), one in effect obtains another solution $n_{11,\mathrm{R}} \neq 0$, i.e., Eq. (80).

It should be mentioned that up to now the runaway speed of the Kaplan turbine has often been given in the form of $n_\mathrm{R}/n_\mathrm{N}$. In [14], for instance, the runaway speeds of the Kaplan turbine have been indicated to be $n_\mathrm{R}/n_\mathrm{N} = 2.0-2.6$ (Kaplan single regulated). First, this indication is much coarse, since the deviation from the median (2.3) is exceedingly high ($\pm 13\%$). Second, the dependence of the runaway speed on the guide-vane settings has not been included.

It should be further mentioned that Eqs. (80) and (81) also apply to the Francis turbine. One only needs to use the respective parameter *S*. In [2], because the reconstructed master equation of using coefficients m_0, m_1 und m_2 had not been given explicitly, the computation of the runaway speed has been expressed in another form. For the computation of the parameter *S*, the ratio $n_{11,\mathrm{R}}/\dot{Q}_{11,\mathrm{R}}$ has been given in [2]. It is very similar to Eq. (78).

The special case of nominal opening of guide vanes is now considered.

From Eq. (78) one obtains

$$S\left(\alpha_{0,\mathrm{N}}\right) = \frac{n_{11,\mathrm{N}}}{\dot{Q}_{11,\mathrm{N}}} + \frac{2d}{\pi b}\frac{1}{\tan\alpha_{0,\mathrm{N}}}\frac{1}{1+r_\mathrm{hub}^2/R^2} \tag{82}$$

The term $\tan\alpha_{0,\mathrm{N}}$ will be replaced by that from Eq. (41). This leads to

$$S\left(\alpha_{0,\mathrm{N}}\right) = \left[\frac{\eta_\mathrm{hyd,N}}{n_{11,\mathrm{N}}^2} + \left(1+\frac{r_\mathrm{hub}^2}{R^2}\right)\right]\frac{n_{11,\mathrm{N}}}{\dot{Q}_{11,\mathrm{N}}}\frac{1}{1+r_\mathrm{hub}^2/R^2} \tag{83}$$

It should be remined that the efficiency $\eta_\mathrm{hyd,N}$ under the nominal operating condition behaves as a given parameter like φ_N and ψ_N. In the considered example in Sect. 2.5, it is $\eta_\mathrm{hyd,N} = 0.9$ according to Table 1. Then, with respect to Eq. (6) and $\psi_\mathrm{N} = 1/n_{11,\mathrm{N}}^2$, one further obtains

$$S\left(\alpha_{0,\mathrm{N}}\right) = \left(1+\frac{\eta_\mathrm{hyd,N}\psi_\mathrm{N}}{1+r_\mathrm{hub}^2/R^2}\right)\frac{4}{\pi}\frac{1}{\varphi_\mathrm{N}} \tag{84}$$

It is now completely related to the turbine runner. Hence, all following computations can also be applied to other types of Kaplan turbines like the bulb turbine, see Sect. 4 below.

While using m_0=0, the coefficient m_1 is likely computed from Eq. (73) with respect to Eq. (41):

$$m_1 = \left[\frac{\eta_\mathrm{hyd,N}}{n_{11,\mathrm{N}}^2} - \left(1+\frac{r_\mathrm{hub}^2}{R^2}\right)\right]\frac{n_{11,\mathrm{N}}}{\dot{Q}_{11,\mathrm{N}}} = \left[\eta_\mathrm{hyd,N}\psi_\mathrm{N} - \left(1+\frac{r_\mathrm{hub}^2}{R^2}\right)\right]\frac{4}{\pi}\frac{1}{\varphi_\mathrm{N}} \tag{85}$$

For the computation of m_2 with $m_2 = k_\mathrm{A}$, it follows from Eq. (62), again with respect to Eq. (6)

$$m_2 = \left(1+\frac{r_\mathrm{hub}^2}{R^2}\right)\frac{n_{11,\mathrm{N}}^2}{\dot{Q}_{11,\mathrm{N}}^2}+\frac{16}{\pi^2}\frac{\zeta_\mathrm{Q}}{\left(1-r_\mathrm{hub}^2/R^2\right)^2}=\left(1+\frac{r_\mathrm{hub}^2}{R^2}\right)\frac{16}{\pi^2}\frac{1}{\varphi_\mathrm{N}^2}+\frac{16}{\pi^2}\frac{\zeta_\mathrm{Q}}{\left(1-r_\mathrm{hub}^2/R^2\right)^2} \tag{86}$$

The question arises whether the approximation $\zeta_\mathrm{Q}=0$ can be applied. The use of the approximation certainly leads to the overestimation of the runaway speed. Because the discharge under the condition of runaway speed is significantly large, see $\dot{Q}_{11}$-curve in Fig. 5, the viscous friction effect ($\zeta_\mathrm{Q}>0$) could be incredibly large. This can be verified through comparison between computations with and without the approximation, respectively. The difference is found only in the coefficient m_2, i.e., the last term in Eq. (86). For the considered computation example, the overestimations of both the runaway speed and the discharge are of about 10%. Obviously, this is unfortunately a bit too large.

Only for the purpose of completeness of theoretical analyses, the outcome of $\zeta_\mathrm{Q}=0$ and hence of $\eta_\mathrm{hyd,N}=1$ is given here. First, one obtains

$$\frac{m_2}{S^2}+\frac{m_1}{S}=\left(\frac{\psi_\mathrm{N}}{1+r_\mathrm{hub}^2/R^2+\psi_\mathrm{N}}\right)^2\left(1+\frac{r_\mathrm{hub}^2}{R^2}\right) \tag{87}$$

$$m_2+m_1 S=\left(\frac{4}{\pi}\frac{\psi_\mathrm{N}}{\varphi_\mathrm{N}}\right)^2\frac{1}{1+r_\mathrm{hub}^2/R^2} \tag{88}$$

Then, it follows from Eqs. (80) and (81), respectively, with m_0=0

$$n_{11,\mathrm{R}}\left(\alpha_{0,\mathrm{N}}\right)=\frac{\sqrt{1+r_\mathrm{hub}^2/R^2}}{\psi_\mathrm{N}}+\frac{1}{\sqrt{1+r_\mathrm{hub}^2/R^2}} \tag{89}$$

$$\dot{Q}_{11,\mathrm{R}}\left(\alpha_{0,\mathrm{N}}\right)=\sqrt{1+\frac{r_\mathrm{hub}^2}{R^2}}\,\frac{\pi}{4}\frac{\varphi_\mathrm{N}}{\psi_\mathrm{N}} \tag{90}$$

When to these two equations the relation $\psi_\mathrm{N}=1/n_{11,\mathrm{N}}^2$ and Eq. (6) are applied, then the runaway speed and discharge, related to the nominal values, are computed as

$$\frac{n_\mathrm{R,N}}{n_\mathrm{N}}=\sqrt{\frac{1+r_\mathrm{hub}^2/R^2}{\psi_\mathrm{N}}}+\sqrt{\frac{\psi_\mathrm{N}}{1+r_\mathrm{hub}^2/R^2}} \tag{91}$$

$$\frac{\dot{Q}_\mathrm{R,N}}{\dot{Q}_\mathrm{N}}=\sqrt{\frac{1}{\psi_\mathrm{N}}\left(1+\frac{r_\mathrm{hub}^2}{R^2}\right)} \tag{92}$$

In the considered example (Fig. 5), these two equations have led to $n_{\mathrm{R,N}}=500$ rpm and $\dot{Q}_{\mathrm{R,N}}=103$ m³/s, respectively. If compared with true values in Table 1, the respective overestimations are about 10% and 12%. As said above, these two values appear to be a bit too large, so that Eqs. (89) to (92), based on the approximation $\zeta_{\mathrm{Q}}=0$, should not be simply used for the Kaplan turbine.

An interesting relation is found, if Eq. (91) is compared with Eq. (77). For $\eta_{\mathrm{hyd,N}}=1$ which is based on $\zeta_{\mathrm{Q}}=0$, one obtains

$$\left.\frac{\mathrm{d}\eta_{\mathrm{hyd}}}{\mathrm{d}n_{11}}\right|_{\mathrm{n=0,N}}=\frac{n_{\mathrm{R,N}}}{n_{\mathrm{N}}}\sqrt{\psi_{\mathrm{N}}} \tag{93}$$

The physical background of this relation, however, is not yet clear.

Another interesting relation is further found, if Eq. (92) is compared with Eq. (65):

$$\frac{\dot{Q}_{\mathrm{R,N}}}{\dot{Q}_{\mathrm{N}}}=\frac{\dot{Q}_{\mathrm{N}}}{\dot{Q}_{\mathrm{n=0,N}}} \quad \text{or} \quad \dot{Q}_{\mathrm{N}}=\sqrt{\dot{Q}_{\mathrm{R,N}}\dot{Q}_{\mathrm{n=0,N}}} \tag{94}$$

The nominal discharge $\dot{Q}_{\mathrm{N}}$ is the geometric mean of the runaway discharge $\dot{Q}_{\mathrm{R,N}}$ and the free-flow discharge $\dot{Q}_{\mathrm{n=0,N}}$.

Other special relations can also be obtained, for instance, from Eq. (71) for $\eta_{\mathrm{hyd,N}}=1$ and Eq. (92).

4 Other Types of Kaplan Turbines

In all computations in Sect. 1, which lead to the establishment of the master equation, the employed control parameter is the guide-vane opening α_0, see Fig. 2. For other forms of the Kaplan turbine, like the bulb turbine and those with guide vanes being placed close to the runner (Fig. 8), the control parameter α_0 can no longer be applied. In order to make further use of all computations in the above sections, a new and equivalent control parameter must be redefined.

For this purpose, the mean radius r_{m} is introduced as the *reference radius*, which divides the flow area into two equal sub-areas $\pi\left(r_{\mathrm{m}}^2-r_{\mathrm{hub}}^2\right)=\pi\left(R^2-r_{\mathrm{m}}^2\right)$. It is then computed as

$$r_{\mathrm{m}}=\sqrt{\frac{R^2+r_{\mathrm{hub}}^2}{2}} \tag{95}$$

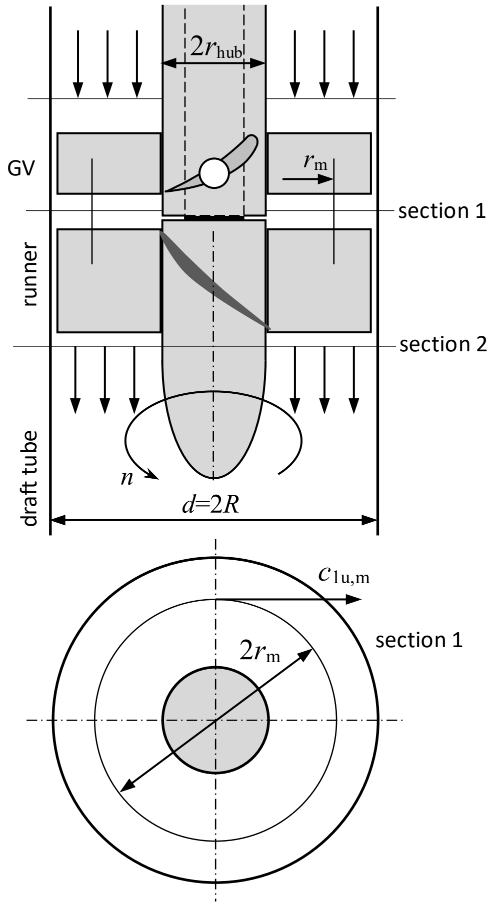

Fig. 8 Kaplan turbine with adjustable guide vanes close to the runner in the same tube

To replace the control parameter α_0, which is found in Fig. 2, one first obtains from Eq. (11)

$$\frac{2b}{R}\tan\alpha_0 = \frac{c_{\mathrm{m}}}{rc_{\mathrm{1u}}}R\left(1-\frac{r_{\mathrm{hub}}^2}{R^2}\right) \tag{96}$$

In all computations carried out in Sect. 1 to Sect. 3, the property of the precise potential flow in the cross-section ahead of the turbine runner has been made use of. At the Kaplan turbine shown in Fig. 8, however, the exact and comparable potential flow distribution could not be obtained at operations outside of the design point (this will be demonstrated below). This determines that interaction between the flow and the turbine runner in case of Fig. 8 differs from that in case of Fig. 2. The flow basically becomes undescribable. For the sake of simplicity of computations, the flow after passing through the guide vanes can still be approximated to be a potential flow. This simply means that the distribution of the circumferential velocity component is describable by the relation $rc_{\mathrm{1u}} = r_{\mathrm{m}}c_{\mathrm{1u,m}}$, with $c_{\mathrm{1u,m}}$ as the velocity component found at the mean radius r_{m}. Then, Eq. (96) is further written as

$$\frac{2b}{R}\tan\alpha_0 = \frac{c_{\mathrm{m}}}{c_{\mathrm{1u,m}}}\frac{R}{r_{\mathrm{m}}}\left(1-\frac{r_{\mathrm{hub}}^2}{R^2}\right) = \tan\alpha_{\mathrm{1m}}\frac{R}{r_{\mathrm{m}}}\left(1-\frac{r_{\mathrm{hub}}^2}{R^2}\right) \tag{97}$$

In principle, the flow angle $\alpha_{1\mathrm{m}}$ in cross-section 1 is determined by the guide-vane angle α_{GVm} at the radius r_{m} on the trailing edge of the blade. With $\alpha_{\mathrm{GVm}} = \alpha_{1\mathrm{m}}$, the above equation is also written as

$$\frac{2b}{R}\tan\alpha_0 = \tan\alpha_{\mathrm{GVm}}\frac{R}{r_{\mathrm{m}}}\left(1-\frac{r_{\mathrm{hub}}^2}{R^2}\right) \tag{98}$$

Correspondingly, there follows for the nominal operating point

$$\frac{2b}{R}\tan\alpha_{0,\mathrm{N}} = \tan\alpha_{\mathrm{GVm,N}}\frac{R}{r_{\mathrm{m}}}\left(1-\frac{r_{\mathrm{hub}}^2}{R^2}\right) \tag{99}$$

In all computations from Sect. 1 to Sect. 3, expressions $(2b/R)\tan\alpha_0$ and $(2b/R)\tan\alpha_{0,\mathrm{N}}$ can be replaced by the respective last terms in the above two equations. In this way, a new control parameter for load regulation is found to be α_{GVm} at the radius r_{m}. Its nominal setting is $\alpha_{\mathrm{GVm,N}}$. All relevant hydraulic characteristics, like that in Figs. 4, 5 and 6, can be computed and redrawn in terms of guide-vane settings α_{GVm}.

In analogy to Eq. (42), the *first design equation* of the current Kaplan turbine can be derived based on the use of design parameter $n_{\mathrm{N}}\dot{Q}_{\mathrm{N}}/gH$. This is obtained from Eqs. (42) and (99):

$$R\tan\alpha_{\mathrm{GVm,N}} = \frac{2}{\eta_{\mathrm{hyd,N}}}\frac{r_{\mathrm{m}}}{R}\frac{1}{1-r_{\mathrm{hub}}^2/R^2}\frac{n_{\mathrm{N}}\dot{Q}_{\mathrm{N}}}{gH} \tag{100}$$

After having selected the hub-diameter ratio r_{hub}/R and hence r_{m}/R, the size of the Kaplan turbine is determined in terms of $R\tan\alpha_{\mathrm{GVm,N}}$.

The concept of designing the guide vanes is again focused to creation of potential flows at the exit of guide-vane channels. The relevant circumferential velocity component and its radial distribution are obtained from Eq. (96) and Eq. (99), both for the nominal operation:

$$\frac{c_{\mathrm{m,N}}}{c_{1\mathrm{u,N}}} = \frac{r}{r_{\mathrm{m}}}\tan\alpha_{\mathrm{GVm,N}} \tag{101}$$

It represents the flow angle in form of $\tan\alpha_{1,\mathrm{N}}$ as a function of the radial coordinate. For blade-congruent flows there must be $\alpha_{1,\mathrm{N}} = \alpha_{\mathrm{GV,N}}$. Thus, one obtains

$$\tan\alpha_{\mathrm{GV,N}} = \frac{r}{r_{\mathrm{m}}}\tan\alpha_{\mathrm{GVm,N}} \tag{102}$$

This is the *design equation* of guide vanes. The twist angle of blades along the blade trailing edge, in form of $\tan\alpha_{\mathrm{GV,N}}$, linearly changes with the radial coordinate.

The fact to be mentioned is that the related design rule only ensures the swirl flow with $c_{1u,N} \propto 1/r$ for the circumferential velocity component under the nominal operating condition. At other operating points in case of load regulation, the desired swirl flow distribution cannot be accurately achieved. This is different from the regulation behaviour of the Kaplan turbine that has been shown in Fig. 2 and considered in previous sections. This can be demonstrated by considering Eq. (102) as follows:

Supposing that the opening of guide vanes is changed by $\Delta\alpha_{GV}$ for the purpose of turbine load regulation. Then, both the distribution angle $\alpha_{GV,N}(r)$ and the fixed angle $\alpha_{GVm,N}$ in Eq. (102) change to $\alpha_{GV,N}+\Delta\alpha_{GV}$ and $\alpha_{GVm,N}+\Delta\alpha_{GV}$, respectively. Because with these two new values Eq. (102) cannot hold and thus becomes invalid, the blade-congruent flow out of the guide vanes is no longer equal to the distribution of a potential flow. This flow dynamics is related to the occurrence of energy losses in the flow while passing through the guide vanes. On the other hand, however, if these losses are negligible, then the exit flow out of guide vanes will tend to be redistributed by itself to meet the potential flow profile ($c_{1u,N} \propto 1/r$). For simplicity of computations, especially for direct applications of all computations performed in Sect. 1 to Sect. 3, potential flow profiles at the exit of guide vanes can still be supposed.

Figure 9 shows the computed velocity distributions, respectively, for the nominal and a partial opening of guide vanes (63% GO). The Kaplan turbine considered is the same as used in Fig. 5 in accordance with Table 1, however, with the guide vanes being placed close to the runner (Fig. 8). Obviously, the exit flow out of the guide vanes with 63% GO has satisfactorily agreed with the profile of potential flows.

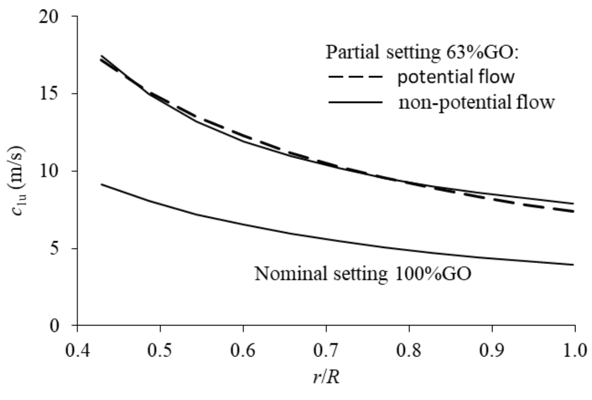

Fig. 9 Velocity profile at the exit of guide vanes of a Kaplan turbine according to Fig.8.

In summary, all computations carried out in Sect. 1 to Sect. 3 can be applied to the current case with adjustable guide vanes according to Fig. 8. One only needs to use the substitutions of Eqs. (98) and (99). The new control parameter is now the guide-vane angle α_{GVm}.

For Kaplan turbines with adjustable runner blades, both the master equation and the runaway speed must be completely recalculated.

5 Summary

The main objective of the current paper is focused on the creation of the master equation of the Kaplan turbine. For better understanding and applications, computations similar to that for the Francis turbine [2] has been completed.

First, the nominal operation of the turbine has been extended to involve the variation of both the hydraulic head and the runner rotational speed. With the introduction of a new design parameter in place of the specific speed, three design equations have been presented for dimensioning the Kaplan turbine and configuring blade profiles.

Furthermore, based on averaging of the Euler equation and accurate computations of both the shock and the swirling losses, two *energy equations* are formed, from which the master equation of the Kaplan turbine has been created. The master equation uniquely combines the geometric design of the turbine runner with the dynamic operations of the turbine unit, so that, for the first time, the complete characteristics of the Kaplan turbine can be analytically computed. The master equation in a reconstructed form, additionally, permits the accurate determination of the runaway speed, explicitly, as a function of the guide-vane settings. Just because of this functional dependence, the computational accuracy is at least one order higher than that found in the literature and handbooks.

All computations leading to the master equation and successive equations can also be applied to the bulb turbine and other types of Kaplan turbines with guide vanes ahead of the turbine runner in the same tube. The corresponding substituting control parameter has been given.

Many special cases like the free flow through the turbine at n=0 have been considered. All simplified relations can be applied to validate designs and CFD simulations. For the latter, then, validations through expenditure experimental measurements would become unnecessary.

The author kindly and appreciatively asks the interested readers or researchers to make validations of the method presented in this paper with their experimental data.

References

[1] Zhang Zh. Pelton Turbines [M]. Cham, Switzerland, Springer-Verlag, 2016.

[2] Zhang Zh. Master equation and runaway speed of the Francis turbine [J]. *J Hydrodyn* 30, 203–217 (2018).

[3] Gieseck, J., Mosonyi E. Wasserkraftanlagen [M]. 6. Auflage, Springer-Verlag, 2014.

[4] Bohl W. Strömungsmaschinen 2 [M]. 8. Auflage, Vogel Fachbuch, 2012.

[5] Quantz L., Meerwarth K. Wasserkraftmaschinen [M]. 11. Auflage, Springer-Verlag, 1963.

[6] Jehle, C. Bau von Wasserkraftanlagen [M]. 6. Auflage, Berlin, Offenbach, VDE Verlag, 2016.

[7] Rai, A., Kumar, A. Analyzing hydro abrasive erosion in Kaplan turbine: A case study from India (J). *J Hydrodyn*, 28, 863-872 (2016).

[8] Tran, C.T., Long, Xp., Ji, B. et al. Prediction of the precessing vortex core in the Francis-99 draft tube under off-design conditions by using Liutex/Rortex method [J]. *J Hydrodyn* 32, 623–628 (2020).

[9] Yang, J., Zhou, Lj. & Wang, Zw. Numerical investigation of the cavitation dynamic parameters in a Francis turbine draft tube with columnar vortex rope [J]. *J Hydrodyn* 31, 931–939 (2019).

[10] Mulu BG., Cervantes MJ., Devals C. et al. Simulation-based investigation of unsteady flow in near-hub region of a Kaplan Turbine with experimental comparison [J]. *Engineering Applications of Computational Fluid Mechanics*, March 2015.

[11] Muntean S., Balint D., Susan-Resiga R. et al. 3D Flow Analysis in the Spiral Case and Distributor of a Kaplan Turbine [C]. 22nd *IAHR Symposium on Hydraulic Machinery and Systems*, Stockholm, Sweden, 2004.

[12] Muntean S., Balint D., Susan-Resiga R. et al. Analytical representation of the swirling flow upstream the Kaplan turbine runner for variable guide vane opening [C]. 23rd *IAHR Symposium on Hydraulic Machinery and Systems*, Yokohama, Japan, 2006.

[13] Zhang Zh. Hydraulic Transients and Computations [M]. Switzerland, Springer-Verlag, 2020.

[14] ESHA. Guide on how to develop a small hydropower plant. European Small Hydropower Association (ESHA), 2004.